Magnetic order of multiferroic $ErMn_2O_5$ studied by resonant soft x-ray Bragg diffraction

U. Staub,[1] Y. Bodenthin,[1] M. García-Fernández,[1,*] R. A. de Souza,[1] M. Garganourakis,[1] E. I. Golovenchits,[2] V. A. Sanina,[2] and S. G. Lushnikov[2]

[1]*Swiss Light Source, Paul Scherrer Institut, CH-5232 Villigen PSI, Switzerland*

[2]*A.F. Ioffe Physical Technical Institute of RAS, 26 Polytechnicheskaya, 194021 St. Petersburg, Russia*

(Received 20 January 2010; revised manuscript received 23 February 2010; published 2 April 2010)

Resonant magnetic soft x-ray diffraction is used to study the magnetic order of the Mn sublattices in multiferroic $ErMn_2O_5$. Data were collected at the Mn $L_{2,3}$ edges as a function of temperature, incident polarization, including the analysis of scattered polarizations for selected azimuths. The energy dependence of the magnetic reflections depends on the azimuthal angle in the commensurate magnetic (CM) ferroelectric (FE) phase, indicating different contributions to the scattering. In the incommensurate magnetic [two-dimensional (2D)-ICM] phase, the two observed reflections $(1/2 \pm \delta_x\ 0\ 1/4+\delta_z)$ have distinct energy dependences too. Different origins of these differences in spectral shape are discussed. The azimuthal angle dependence at the L_3 edge can only be qualitatively described by a generalized magnetic model. The observed discrepancies may indicate the importance of magnetoelectric multipole scattering to these reflections. Reciprocal mesh scans show diffuse scattering along **q** and perpendicular to **q** as well as along the $(h\ 0\ 0)$ direction in the CM phase. Diffuse scattering is also observed along $(h\ 0\ 0)$ in the one-dimensional-ICM phase. At higher temperatures, in the 2D-ICM phase, the diffuse magnetic scattering is almost isotropic.

DOI: 10.1103/PhysRevB.81.144401 PACS number(s): 75.85.+t, 75.25.−j

I. INTRODUCTION

The magnetoelectric effect regained strong interest in recent years due to the observation of strong coupling between magnetic phase transitions and the occurrence of a spontaneous electric polarization. In particular, magnetic systems with frustrated magnetic interactions such as the $RMnO_3$ and RMn_2O_5 family (R=rare-earth ion) were shown to have huge couplings between ferroelectricity and magnetism.[1,2] The application of magnetic fields may affect strongly the ferroelectric properties and also, though much smaller, effects on applied electric fields were observed on the magnetic properties.[3–8] By the application of an electric field during cooling through the ferroelectric transition, a single defined chiral magnetic state can be selected in $TbMnO_3$.[6] In the $ErMn_2O_5$, strong electric fields perpendicular to the ferroelectric moment affect the commensurate magnetic structure.[7] There is additional induced intensity of the commensurate magnetic (1/2 0 1/4) reflection and even an observed hysteric behavior of the intensity versus applied electric field.

The RMn_2O_5 system exhibits a variety of magnetic phases with complex incommensurate and noncollinear commensurate phases. Interesting is the presence of a ferroelectric polarization in the commensurate phase. The magnetic order has been studied in detail with neutron[9–14] and resonant x-ray diffraction.[15–18] The order parameters and the magnetic phase diagram have also recently been investigated by theory including symmetry considerations.[19,20] Independent of the R ion, the first magnetic phase transition enters into an incommensurate magnetic phase [two-dimensional (2D)-ICM] upon cooling followed by two successive transitions to a ferroelectric (FE) incommensurate [one-dimensional (1D)-ICM] and to a FE commensurate (CM) phase. At lower temperatures, an additional incommensurate magnetic phase (LT-ICM) occurs.

In the paramagnetic phase, the material contains Mn^{3+} in square pyramid type oxygen coordination and Mn^{4+} in a distorted octahedral coordination. In addition, most trivalent R ions are magnetic and can play a significant role due to the Mn-R exchange and the strong anisotropy of the magnetic f shell. For R=Ho, Tb, and Dy, the magnetic easy axis is expected to be in the a,b plane whereas for Er, it is perpendicular to it based on the expected different sign of the B_0^2 crystal-field parameters.

Resonant x-ray diffraction has become a powerful technique to study magnetic and electronic ordering phenomena, and has been applied to several RMn_2O_5 systems.[7,15–18] Soft x rays, which have the advantage to couple directly to the Mn $3d$ and R $4f$ states, have been used for Tb (Refs. 17 and 18) and Er.[7] However, part of the results on Tb is not consistent. The observed energy dependence of the magnetic reflection at the Mn $L_{2,3}$ edge is very different between the two studies. In the first study,[17] the temperature dependence of the commensurate reflection was interpreted as being related to the electric polarization in a simple manner. The second study found a different temperature dependence of the incommensurate reflections at different energies in the vicinity of the Mn $L_{2,3}$ edges,[18] complicating a simple relation between observed magnetic intensities and the electric polarization. Different temperature dependences of individual spectral features of the Bragg intensities were interpreted in terms of the existence of different order parameters. Such observations have also been used to distinguish different order parameters of the orbital reflection in $La_{0.5}Sr_{1.5}MnO_4$.[21]

To clarify some of these issues, we performed a resonant soft x-ray diffraction study to elucidate the origin of the different incommensurate superlattice reflections observed at the Mn $L_{2,3}$ edge of $ErMn_2O_5$. It is shown that the two different incommensurate reflections have significant different energy dependence, indicative of different contributions to the reflections. In the commensurate phase, the different en-

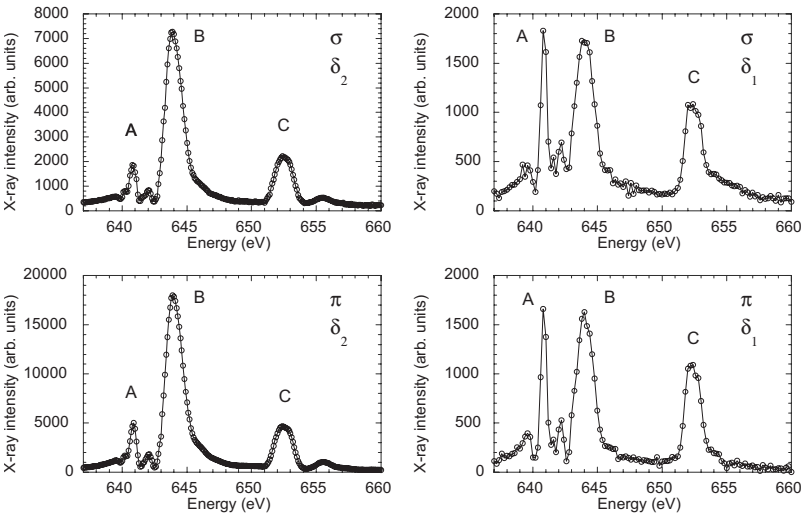

FIG. 1. Energy dependences of the incommensurate satellite reflections δ_1 and δ_2 with 39 K over the Mn $L_{2,3}$ edges for both σ and π incident radiation and at azimuthal angle $\psi=0°$. No polarization analysis is applied to the outgoing radiation.

ergy dependence observed in the ICM phase is recovered at different azimuthal angles. Polarization analysis did not find any intensity in the σ-σ' scattering channel, consistent with a magnetic origin of both reflections. The azimuthal angle dependence shows the absence of an m_z contribution in the structure factor but only with a qualitative agreement with a model based on a general magnetic structure.

II. EXPERIMENT

A single crystal of $ErMn_2O_5$ has been grown by spontaneous crystallization.[22] The crystal has been characterized with Cu $K\alpha$ radiation. Resonant magnetic soft x-ray diffraction experiments have been performed at the RESOXS endstation at the SIM beamline of the Swiss Light Source at the Paul Scherrer Institut. Measurements were carried out in horizontal scattering geometry at the Mn $L_{2,3}$ edges. The sample was glued on an aluminum plate and was cooled to temperatures between 10 and 50 K using a helium-flow cryostat. The linear polarization of the incident radiation was either horizontal (π) or vertical (σ). Polarization analysis of the scattered radiation was performed using a graded W/C multilayer setup.[23,24] Rotations around the Bragg wave vector (azimuthal angle ψ) used the rotatable sample transfer fork with accuracy better than five degrees. An angle of zero degree reflects the situation of [010] direction lying in the horizontal scattering plane.

III. RESULTS

A. Energy dependence of Bragg reflections

Two reflections have been observed by resonant soft x-ray diffraction at the Mn $L_{2,3}$ edges in the 1D-ICM and 2D-ICM phases of $ErMn_2O_5$.[7] Both have significant different intensities and different temperature dependence. They were labeled with δ_1 (δ) and δ_2 (-2δ). Interestingly, only the δ_1 type peak was observed with neutron diffraction,[9] which led to the suggestion that the δ_2 may reflect the magnetic-induced charge anisotropy appearing at the double of the incommensurate wave vector. The fact that these two incommensurate satellite reflections are of different origin is supported by their distinct different energy dependences, which are shown in Fig. 1. Figure 1 shows that the energy dependences of both satellites does not depend on the incident x-ray polarization (σ and π), at least for this particular $\psi=0°$. This indicates either a dominant component of scattering contributing to the reflection or that the contributions add coherently. Figure 2 shows the energy dependence of the commensurate (1/2 0 1/4) reflection in the CM phase at an azimuthal angle of $\psi=-30°$ for σ and π incident polarization together with the absorption data taken in total fluorescence mode. In

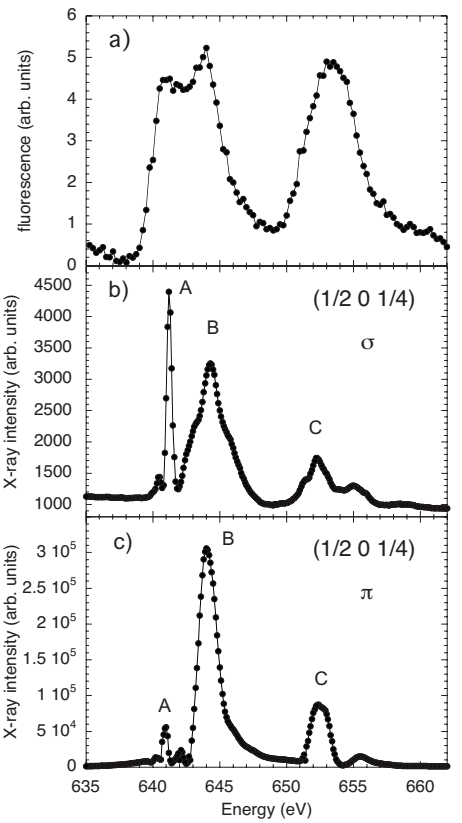

FIG. 2. (a) Fluorescence scan and energy dependence of the (1/2 0 1/4) reflection taken with (b) σ and (c) π incident radiation at the azimuthal angle of $\psi=-30°$ taken at 30 K in the CM phase.

contrast to the incommensurate satellite reflections the spectra with different incoming polarization have very different energy dependences, giving clear evidence of a multicomponent structure. The spectra taken with σ and π polarization bear significant resemblance to those of δ_1 and δ_2, respectively, despite the fact that they have been taken with significant better energy resolution. Note that also for the $\psi=0°$, the CM reflections has different spectral shape for σ and π incident polarization but the difference is less pronounced (not shown). Moreover the stronger signal provides data with significant better signal-to-noise ratio. This allows us to detect additional salient features in the energy dependences. Energy scans at other azimuths have smaller differences between the two different incoming polarization channels, in both, energy shape and overall intensities. Therefore, the azimuthal angle of $\psi=-30°$ corresponds to a position where the δ_2 contribution to the commensurate reflections for the σ channel is strongly suppressed and the scattering is dominated by the weaker δ_1 contribution, whereas for the π channel, the δ_2 contribution, which is already much stronger in the ICM phases, dominates.

The energy dependence of the commensurate reflection at the Mn $L_{2,3}$ edges is significantly different compared to those found for $TbMn_2O_5$, although the fluorescence looks very similar. The energy dependence of these reflections resembles more that found by Koo *et al.*,[18] with similar spectral features but different intensities. There is barely any resemblance to that found by Okamoto *et al.*[17] where particular strong magnetic intensities were observed between the Mn $L_{2,3}$ edges. A possible reason for this large discrepancy with Ref. 17 might be a strong absorption effect caused by a magnetic dead layer at the surface leading to a minimum in the energy dependence where absorption is strongest. Note that even though the energy scan does not likely represent the intrinsic energy dependence of the magnetic reflection, it does probably not affect the presented temperature evolution of momentum and intensity behavior. None of the energy spectra observed for $ErMn_2O_5$ have a consistent spectral shape with those obtained for $TbMn_2O_5$.[17,18] The differences compared to Ref. 18 are an indication that the magnetic structure for the two different RMn_2O_5 systems is different. It might reflect different magnetic-moment directions of spins at the Mn sites causing the magnetic structure factor to have different contributions of the moments of Mn^{3+} and Mn^{4+}. Note that the energy dependence of the magnetic scattering factors of the different valence states inherently differ from each other but the energy dependence is usually assumed to be independent of the moment direction.

B. Temperature dependence

The energy dependence of the commensurate magnetic reflection (1/2 0 1/4) as a function of temperature is shown for the two different incident polarization channels π and σ in Fig. 3. At the lowest temperature, at the border to the incommensurate (LT-ICM) phase, the first strong and sharp spectral feature is largest in the incident σ channel. For increasing temperatures, the ratio of the intensity of this sharp feature A (640.8 eV) compared to the feature around B (644 eV) or that at the L_2 edge C (652.6 eV) is strongly decreasing. For the π channel, this ratio I_A/I_B changes slightly too, but with opposite dependence, and slightly increases for increasing temperatures. This behavior is indicative of changes in the magnetic structure in the commensurate phase. These changes might reflect the different contributions of the magnetic moments from the Mn^{3+} and Mn^{4+} ions, caused by a rotation of these moments. However, this does not necessary mean that these moments have a different temperature dependence. It may indicate that the individual moments change their direction in addition to their value and correspondingly contribute differently to the structure factor. Interesting is also the observation that for decreasing temperatures below 30 K the intensity of feature B is again decreasing for σ incident polarization, in contrast to the respective spectral feature with π incident radiation, where it continues to increase. The temperature dependence of the incommensurate magnetic reflections of $TbMn_2O_5$ taken at the different spectral features are also very different.[18] There, however, these differences occur mainly in the low-temperature incommensurate magnetic phase. Again, this does not necessary indicate multiple magnetic order parameters of Mn ions in the system.

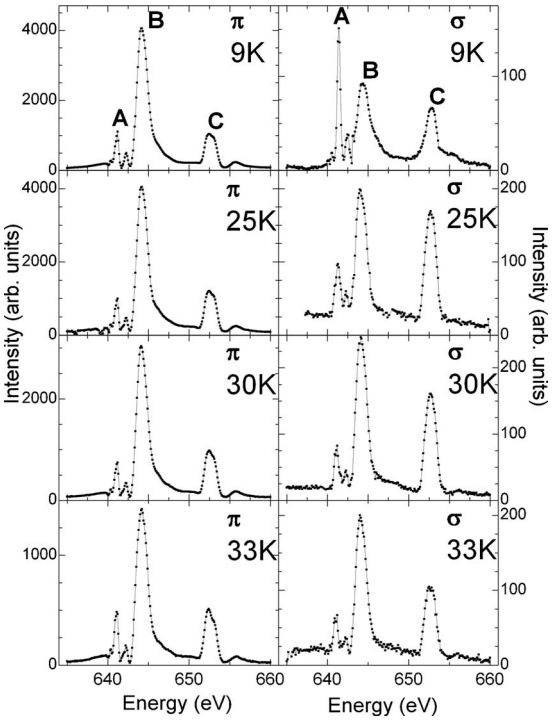

FIG. 3. Energy scan of the (1/2 0 1/4) reflection for different temperatures and incident x-ray polarizations taken at $\psi=-45°$.

C. Momentum dependence of reflections

To understand more about the origin of the two satellite reflections in the high-temperature ICM regimes, we scanned the reciprocal space and collected the scattered intensity for different temperatures. These reciprocal space maps are shown in Fig. 4(a) for the commensurate phase, Fig. 4(b) for the 1D-ICM phase, and Figs. 4(c) and 4(d) for the 2D-ICM

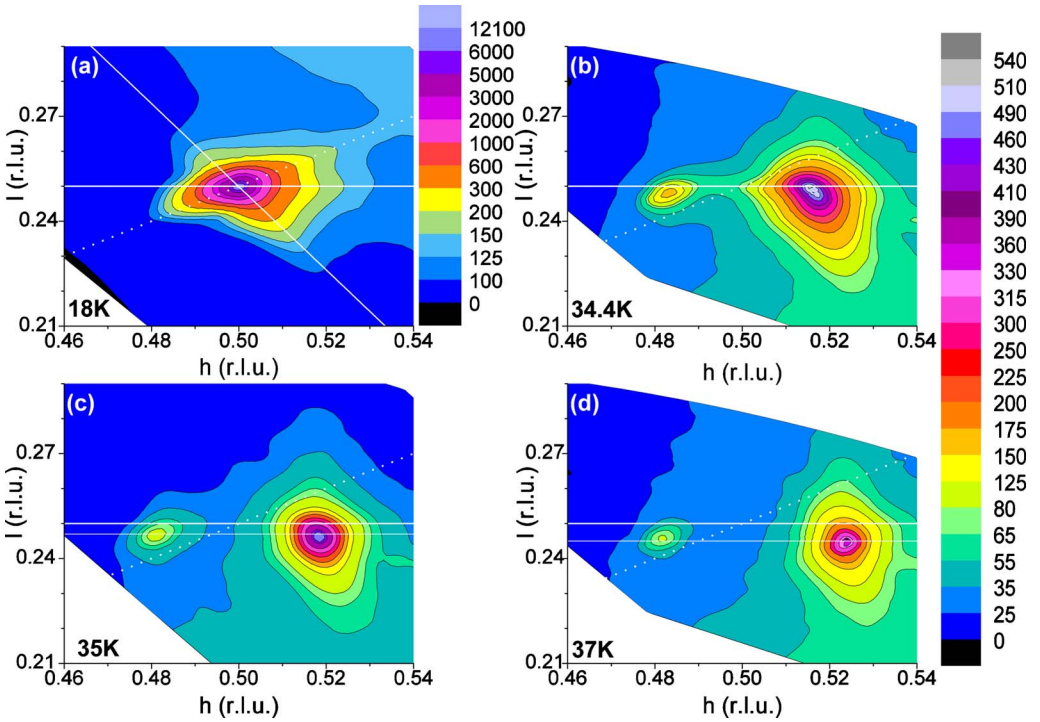

FIG. 4. (Color online) X-ray intensity maps in reciprocal space around the magnetic (1/2 0 1/4) reflection taken at L_3 edge at 644 eV with π incidence and $\psi=90°$ (having the b axis perpendicular to the scattering plane). The (white) solid lines visualize particular directions in reciprocal space perpendicular or parallel and perpendicular to the momentum transfer where diffuse scattering trails are observed. The thin solid horizontal line visualize the deviation from the commensurate $l=1/4$ position and the dotted line represents the $(h/2\ 0\ h/4)$ direction.

phase. In the commensurate phase at $T=18$ K, there is a single reflection observed, in contrast to $TbMn_2O_5$,[17] where the ICM reflections were still present but weak. Here we observe though diffuse scattering along (h 0 1/4) and interestingly also parallel and perpendicular to ordering wave vector in the plane with $k=0$. Note that to obtain the intrinsic width along **q**, marked as a dotted line in the figures, the limited penetration length of the x rays at resonance contributes to the broadening. At $T=34.4$ K, the commensurate reflections split into two reflections of type $(1/2 \pm \delta_h\ 0\ 1/4)$. The commensurate q_z value indicates that the material is in the 1D-ICM phase. Note that the reflections where previously[7] incorrectly assigned to be of magnetic and quadrupole origin. Moreover, in this study the temperatures are taken from the temperature sensor in contrast to the previous experiments,[7] where the temperature was adjusted to match the phase transitions of Ref. 9. The magnetic phase-transition temperatures presented here are consistent with those of Ref. 25, which deviate from those in Ref. 9. For $T=35$ K, the diffuse tail along (h 0 1/4) is almost disappeared and at 37 K, the shape changes to be almost isotropic. The δ_1 $(1/2-\delta_h\ 0\ 1/4-\delta_l)$ type reflection might not have been observed with neutron scattering due to its weakness. Note, however, that the structure factor for neutron diffraction is not the same as for resonant x-ray Bragg diffraction and correspondingly a weak x-ray reflections might not be weak in the neutron-scattering case and vice versa.

D. Azimuthal angle dependence

Further information on the different contributions to the (1/2 0 1/4) reflection (CM phase) can be obtained from its azimuthal dependence ψ, the rotation of the sample around the Bragg wave vector, which is shown in Fig. 5. The ψ dependence has been collected at the main spectral feature B

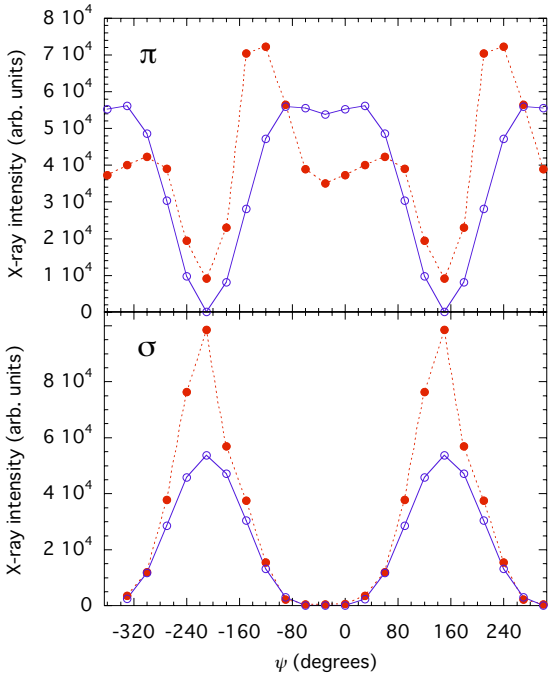

FIG. 5. (Color online) Azimuthal angle dependence of the (1/2 0 1/4) magnetic commensurate reflection taken at 644 eV (feature B). The filled circles represent the experiment and the open circles the calculations as described in the text. The lines guide the eyes.

at 644 eV for both σ and π incident polarizations. An extended low intensity region is observed in the σ channel for $-90° < \psi < 30°$ and a peak maxima at $\psi = 150°$ where the intensity in the π channel is evanescent.

The variation in the diffraction amplitude in an azimuthal scan at resonance for an electric-electric dipole transition is given by

$$F(\theta) = \sum_{Kq} (-1)^q \mathbf{X}^K_{-q}(\theta) \sum_{q'} D^K_{q'q}(\gamma_0, \beta_0, \alpha_0) \mathbf{\Psi}^K_{q'}. \quad (1)$$

The angles $\alpha_0, \beta_0, \gamma_0$ are related to the Euler angles of the rotation that aligns the Bragg vector τ along the $-a$ axis. $\mathbf{\Psi}^K_q$ is the tensor associated with the electrons and is given by the expression $\mathbf{\Psi}^K_q = \Sigma_d e^{i\mathbf{Q}\cdot\mathbf{d}} \langle \mathbf{T}^K_q \rangle_\mathbf{d}$ in which the sum over d runs over all the resonant ions in the unit cell and where $\mathbf{d}$ is the position of the ions within the unit cell. $D^K_{qq'}(\alpha_0, \beta_0, \gamma_0)$ are the Wigner functions that correspond to the matrix elements of the rotations in the angular momentum representation[26] and K is the rank of the tensor. A tensor with rank $K=1$ represents the origin of magnetic scattering. A general model not specifying further the magnetic structure with ordering wave vector (1/2 0 1/4), as applied for the interpretation of a magnetic reflection of the layered cobaltate,[27] is used. Here we describe the σ and π incident polarization scans separately and not their ratio. Since they show clear minima with intensities close to zero, the ratio thus is not an appropriate quantity for the analysis. The expression $\Psi^K_{\pm q}$ reflects the sum of the magnetic-moment components along the different axis weighted by the crystallographic phase factor $\Psi^1_0 \equiv m_z$, $\Psi^1_x = \frac{1}{\sqrt{2}}(\Psi^1_{-1} - \Psi^1_{+1}) \propto m_x$, and $\Psi^1_y = \frac{i}{\sqrt{2}}(\Psi^1_{-1} + \Psi^1_{+1}) \propto m_y$. A fit to the parameters m_x, m_y, and m_z, is also shown in Fig. 5. The fit describes qualitatively the azimuthal angle dependence, in particular, the minima are correctly reproduced. The fit results in values of $m_x \approx -m_y$ and $m_z \approx 0$. One azimuthal scan is obviously not sufficient to determine the magnetic structure, but gives however important information on the sum of the components, which could be used to test the magnetic structure. The value $m_z \approx 0$ does not necessarily imply that all the individual z components of the Mn moments are zero. Nevertheless, it directly shows that the assumption made by Okamoto *et al.*[17] on the z component of $S_q = \Sigma_\mathbf{d} \vec{S}_\mathbf{d} e^{i\mathbf{Q}\cdot\mathbf{d}}$, with $\vec{S}_\mathbf{d}$ being spin moments of the ion with position $\mathbf{d}$, would also apply to the Er case, even though Er is supposed to induce a significant z component on the individual magnetic moments, which is confirmed by neutron diffraction.[14] The agreement of the fit to the azimuthal angle dependence is worse than expected. For I_π the two observed peaks have unequal intensities, which is not reproduced and the intensity is underestimated. Though different values of m_x, m_y, and m_z can lead to an unequal peak intensity for π incidence, it also introduces significant intensity between $-80 < \psi < 0$ in the σ channel, inconsistent with the observations. Introducing an orbital contribution in the same manner as for the magnetic contribution does not significantly improve the fit. A further possibility would be that there are additional contributions of magnetoelectric multipoles through different scattering events, such as E1-M1 as recently observed in $GaFeO_3$.[28]

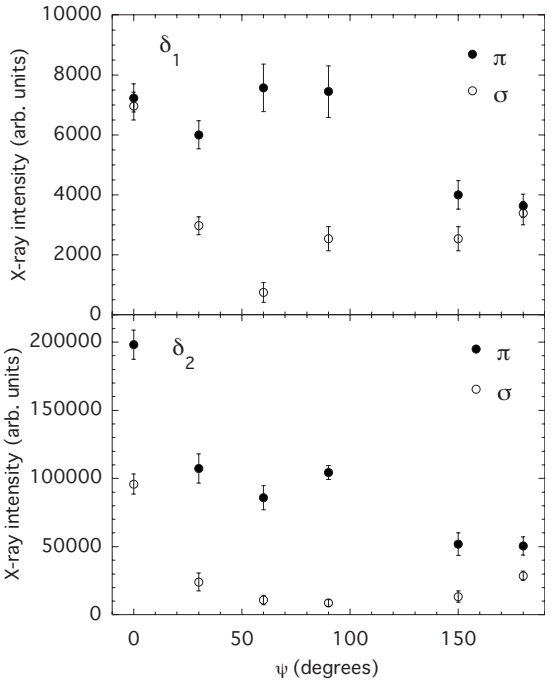

FIG. 6. Azimuthal angle dependence of the two satellite reflections δ_1 and δ_2 observed in the 2D-ICM phase at $T = 37$ K and 644 eV.

Yet, the magnetic and crystal structures are too complex to test such a scenario with the data at hand.

The azimuthal angle dependences of the incommensurate reflections in the 2D-ICM phase are shown in Fig. 6. These intensities are much less reliable, in particular, for the weak δ_1 reflection, as the alignment is difficult when a stronger reflection δ_2 is nearby. Nevertheless, they seem to have similar dependences. This can be cross-checked by comparing the ratio of I_π / I_σ for the two reflections (see Fig. 7). When considering the ratio, most errors from beam/sample shape and misalignment cancel. Again, the ratio of the two reflections follows a similar trend. This makes unlikely that δ_1 and δ_2 represent merely the difference and sum of the Mn^{3+} and Mn^{4+} moments squared, respectively.

E. Polarization dependence

In case of having different contributions to the scattering, experiments with polarization analysis of the scattered radia-

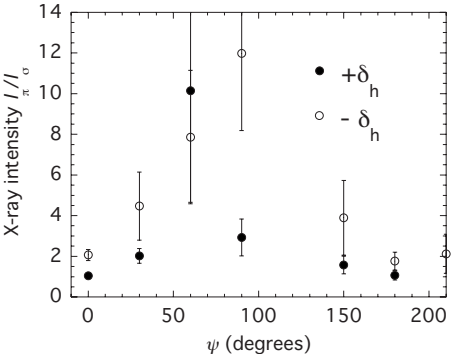

FIG. 7. Ratio of the of x-ray intensity of I_σ / I_π of the reflections $(1/2 \pm \delta_h \; 0 \; 1/4 - \delta_l)$ at temperatures within the (2D-ICM) phase.

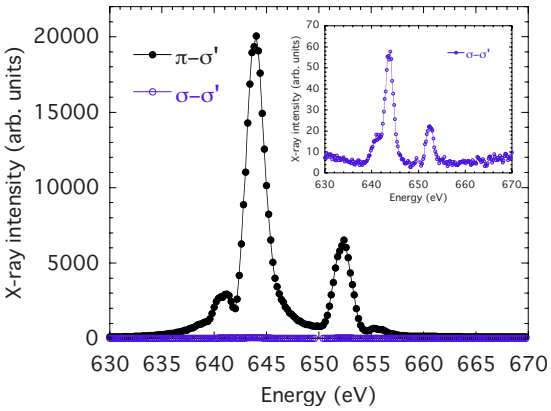

FIG. 8. (Color online) Energy scan of the (1/2 0 1/4) reflection using polarization analysis of the scattered radiation at $T=30$ K and $\psi=30°$. Inset: energy dependence with enlarged y scale of the σ-σ' channel.

tion are very useful and have also been performed recently in the soft x-ray regime.[23,24,27,29] Figure 8 shows the energy scan of the magnetic reflection in the commensurate phase (1/2 0 1/4) with fixed exit polarization σ' and variable incident polarization, σ and π. No intensity (expected leakage in the order of a few ‰) could be observed in the σ-σ' channel. This is also the case for azimuthal angles $0° \leq \psi \leq 120°$. The absence of intensity in the unrotated channel is consistent with pure magnetic origin of the reflection because magnetic scattering is inherently forbidden in the σ-σ' channel.[30] In systems for which inversion symmetry is absent, as under consideration here, orbital (anisotropy of tensor susceptibility) scattering occurs in all four polarization channels. Therefore, an orbital contribution to the CM reflection can be discarded.

IV. DISCUSSION

A recent neutron study, combining single-crystal neutron diffraction with neutron polarimetry, has solved the magnetic structure of $ErMn_2O_5$.[14] This study demonstrated that not only the Er magnetic moments have a component along the z axis but also the Mn moments. Therefore, a comparison of the electric polarization with the x-ray intensities for different polarizations, as performed by Okamoto *et al.*[17] for $TbMn_2O_5$ is not necessary meaningful for $ErMn_2O_5$. The recent determination of the magnetic structure allowed us to calculate the weighted (by the structure factor) sum of the moments for the m_x, m_y, and m_z components [Eq. (1)] which were used in the fit of the general model of the azimuthal angle dependence. For this purpose we assume that at the probed x-ray energy, the magnetic scattering factors of the Mn^{3+} and Mn^{4+} ions scale both equally with the size of the magnetic moment and are equal for equal sizes of the magnetic moments. The obtained values strongly deviate from those from fit with $m_x > m_y$ and m_z significantly nonzero. This behavior is maybe related to the disagreements of the observed azimuthal angle dependence with the general model. This indicates that there are additional contributions to the scattering, which are of nondipole magnetic origin. However, such a comparison does not take into account the unknown scale factor between the Mn^{3+} and Mn^{4+} contributions for a resonant process. The ratio and sign depend on the probed energy (since the magnetic scattering factors have different energy dependence) and likely does not simply reflect the phases-factor weighted sum of the individual magnetic moments.

The other unresolved issue in the presented experimental data is the different energy scans of the two incommensurate satellite reflections and the fact that the spectral shape of the commensurate reflection depends on the azimuthal angle. This observation can either be caused by the fact (a) that the energy spectra of the magnetic scattering factors for Mn^{3+} and Mn^{4+} differ or (b) that there is an additional multipolar component contributing to these scattering process. Option (a) would be consistent with the presented polarization analysis, which did not show a σ'-σ component in the CM (1/2 0 1/4) reflection. But this option cannot explain why the general model failed to describe the azimuthal angle dependence. Note that the different electronic origin of the two moments is not relevant for this model, as it does not contain any assumptions on the exact magnetic or electronic structure except its ordering wave vector (Bragg angle of reflection and axis orientations). If these deviations are caused by an additional multipolar component, it is not likely an electric quadrupole (orbital) moment, as this did not improve the azimuthal angle fit. More likely would be that it reflects a contribution of magnetoelectric multipole moments as discussed in recent literature and has recently been observed in $GaFeO_3$ with resonant soft x-ray diffraction.[28] Such multipoles can be nonzero in systems (at atomic sites) with the absence of inversion symmetry, which is the case for multiferroics. An observation requires though a different scattering event such as mixed electric-magnetic dipole or mixed electric dipole—quadrupole transition. An analysis based along such lines requires the exact symmetry of the low-temperature crystal structure in the ferroelectric phase. Moreover, with the complexity of the magnetic structure of the material, such an interpretation is not straightforward and clearly beyond the present study here.

V. CONCLUSION

Resonant soft x-ray diffraction was used to study the magnetic structure of the Mn sublattice of multiferroic $ErMn_2O_5$. The different energy dependence of the two incommensurate satellite reflections $(1/2 \pm \delta_h\ 0\ 1/4 + \delta_l)$, as well as the different spectral shape depending on the azimuthal angle of the commensurate reflection (1/2 0 1/4) reflection, is caused by either the individual spectral shapes of the magnetic Mn^{3+} and Mn^{4+} scattering factors or by additional magnetoelectric moment contributions. The second possibility is supported by the inability to quantitatively describe the azimuthal angle dependence by a general magnetic model, which is independent of the detailed spin structure. A directional change in diffuse magnetic scattering is observed around the 1D-ICM-2D-ICM phase transition, reflecting the magnetic structural instabilities caused by the competing exchange interactions causing magnetic frustration.

ACKNOWLEDGMENTS

We have benefited from valuable discussions with S. W. Lovesey, S. Gvasaliya, B. Roessli, and M. Janocheck and from the experimental support of the X11MA beamline staff. The work was partially support by the Russian Foundation for Basic Research Grant No. 08-02-00077 and by Presidium of Russian Academy of Sciences Programme 03. The financial support of the Swiss National Science Foundation is grateful acknowledged.

*Present address: Institut de Physique, Université de Fribourg, CH-1700 Fribourg, Switzerland.

[1] T. Kimura, T. Goto, H. Shintani, K. Ishizaka, T. Arima, and Y. Tokura, Nature (London) **426**, 55 (2003).
[2] N. Hur, S. Park, P. A. Sharma, J. S. Ahn, S. Guha, and S.-W. Cheong, Nature (London) **429**, 392 (2004).
[3] E. Ascher, H. Rieder, H. Schmidt, and H. Stössel, J. Appl. Phys. **37**, 1404 (1966).
[4] T. Lottermoser, T. Lonkai, U. Amann, D. Hohlwein, J. Ihringer, and M. Fiebig, Nature (London) **430**, 541 (2004).
[5] T. Zhao, A. Scholl, F. Zavaliche, K. Klee, M. Barry, A. Doran, M. P. Cruz, Y. H. Chu, C. Ederer, N. A. Spaldin, R. R. Das, D. M. Kim, S. H. Baek, C. B. Eom, and R. Ramesh, Nature Mater. **5**, 823 (2006).
[6] Y. Yamasaki, H. Sagayama, T. Goto, M. Matsuura, K. Hirota, T. Arima, and Y. Tokura, Phys. Rev. Lett. **98**, 147204 (2007).
[7] Y. Bodenthin, U. Staub, M. García-Fernández, M. Janoschek, J. Schlappa, E. I. Golovenchits, V. A. Sanina, and S. G. Lushnikov, Phys. Rev. Lett. **100**, 027201 (2008).
[8] P. G. Radaelli, L. C. Chapon, A. Daoud-Aladine, C. Vecchini, P. J. Brown, T. Chatterji, S. Park, and S.-W. Cheong, Phys. Rev. Lett. **101**, 067205 (2008).
[9] S. Kobayashi, T. Osawa, H. Kimura, Y. Noda, I. Kagomiya, and K. Kohn, J. Phys. Soc. Jpn. **73**, 1031 (2004).
[10] H. Kimura, Y. Kamada, Y. Noda, K. Kaneko, N. Metoki, and K. Kohn, J. Phys. Soc. Jpn. **75**, 113701 (2006).
[11] W. Ratcliff, V. Kiryukhin, M. Kenzelmann, S.-H. Lee, R. Erwin, J. Schefer, N. Hur, S. Park, and S.-W. Cheong, Phys. Rev. B **72**, 060407(R) (2005).
[12] P. P. Gardner, C. Wilkinson, J. B. Forsyth, and B. M. Wanklyn, J. Phys. C **21**, 5653 (1988).
[13] C. Vecchini, L. C. Chapon, P. J. Brown, T. Chatterji, S. Park, S.-W. Cheong, and P. G. Radaelli, Phys. Rev. B **77**, 134434 (2008).
[14] B. Roessli, P. Fischer, P. J. Brown, M. Janoschek, D. Sheptyakov, S. N. Gvasaliya, B. Ouladdiaf, O. Zaharko, E. Golovenchits, and V. Sanina, J. Phys.: Condens. Matter **20**, 485216 (2008).
[15] G. Beutier, A. Bombardi, C. Vecchini, P. G. Radaelli, S. Park, S.-W. Cheong, and L. C. Chapon, Phys. Rev. B **77**, 172408 (2008).
[16] R. A. Ewings, A. T. Boothroyd, D. F. McMorrow, D. Mannix, H. C. Walker, and B. M. R. Wanklyn, Phys. Rev. B **77**, 104415 (2008).
[17] J. Okamoto, D. J. Huang, C.-Y. Mou, K. S. Chao, H.-J. Lin, S. Park, S.-W. Cheong, and C. T. Chen, Phys. Rev. Lett. **98**, 157202 (2007).
[18] J. Koo, C. Song, S. Ji, J. S. Lee, J. Park, T.-H. Jang, C.-H. Yang, J.-H. Park, Y. H. Jeong, K.-B. Lee, T. Y. Koo, Y. J. Park, J.-Y. Kim, D. Wermeille, A. I. Goldman, G. Srajer, S. Park, and S.-W. Cheong, Phys. Rev. Lett. **99**, 197601 (2007).
[19] A. B. Harris, A. Aharony, and O. Entin-Wohlman, Phys. Rev. Lett. **100**, 217202 (2008).
[20] A. B. Harris, M. Kenzelmann, A. Aharony, and O. Entin-Wohlman, Phys. Rev. B **78**, 014407 (2008).
[21] U. Staub, V. Scagnoli, A. M. Mulders, M. Janousch, Z. Honda, and J. M. Tonnerre, Europhys. Lett. **76**, 926 (2006).
[22] V. A. Sanina, L. M. Sapozhinkova, E. I. Golovenchits, and N. V. Morozov, Sov. Phys. Solid State **30**, 1736 (1988).
[23] U. Staub, V. Scagnoli, Y. Bodenthin, M. García-Fernández, R. Wetter, A. M. Mulders, H. Grimmer, and M. Horisberger, J. Synchrotron Radiat. **15**, 469 (2008).
[24] U. Staub, V. Scagnoli, A. M. Mulders, K. Katsumata, Z. Honda, H. Grimmer, M. Horisberger, and J. M. Tonnerre, Phys. Rev. B **71**, 214421 (2005).
[25] D. Higashiyama, S. Miyasaka, and Y. Tokura, Phys. Rev. B **72**, 064421 (2005).
[26] S. W. Lovesey, E. Balcar, K. S. Knight, and J. Fernández-Rodríguez, Phys. Rep. **411**, 233 (2005).
[27] M. García-Fernández, V. Scagnoli, U. Staub, A. M. Mulders, M. Janousch, Y. Bodenthin, D. Meister, B. D. Patterson, A. Mirone, Y. Tanaka, T. Nakamura, S. Grenier, Y. Huang, and K. Conder, Phys. Rev. B **78**, 054424 (2008).
[28] U. Staub, Y. Bodenthin, C. Piamonteze, M. García-Fernández, V. Scagnoli, M. Garganourakis, S. Koohpayeh, D. Fort, and S. W. Lovesey, Phys. Rev. B **80**, 140410(R) (2009).
[29] V. Scagnoli, U. Staub, A. M. Mulders, M. Janousch, G. I. Meijer, G. Hammerl, J. M. Tonnerre, and N. Stojic, Phys. Rev. B **73**, 100409(R) (2006).
[30] S. W. Lovesey and S. P. Collins, *X-Ray Scattering and Absorption by Magnetic Materials* (Clarendon Press, Oxford, 1996).